Field Analysis of Rectangular Waveguide Open Junction

Christos T. Iatrou and Marco Cavenago

***Abstract*—The problem of a rectangular waveguide open junction is investigated using field theory and the relevant model of two normally intersected, infinite parallel-planes waveguides. Evanescent waveguide modes generated by waveguide wall edges and/or the discontinuity in dielectric are taken into account; an infinite set of equations is derived, where the mode coupling is given by the dielectric slab modes. Proper pole handling is discussed, and a solution for the system is given. Expressions are derived for the reflected, transmitted, and radiated power, which are shown to be sufficiently reliable in the domain of practical interest, regarding the width and the dielectric loading of the gap. The analysis shows that a substantial fraction of the microwave power leaks from the dielectric gap, confirming the absolute necessity of using a choke-flange at the waveguide junction.**

I. Introduction

FREQUENTLY the microwave coupling of two sections of a waveguide line is desired under circumstances that make the attainment of a good metallic contact difficult or that even prohibit the contact for electrical insulation reasons. A number of applications require this type of coupling, such as rotary joints and other types of motional joints frequently used in radar applications, open junctions allowing possible misalignments in the RF-line components, and dc breaks for dc electrical insulation between two parts of the RF circuit without interrupting the RF signal. In particular, in electron cyclotron resonance ion sources (ECRIS) [1]–[3], the vessel is biased to a high potential of 10÷20 kV, while the klystron amplifier, which feeds the plasma chamber with RF power, and all the components of the RF line up to the chamber are earthed for economy and safety reasons. Thus, the waveguide line must be electrically broken, at a certain position before the plasma chamber, using a dc break [2].

In the literature on the similar problem of open waveguides [4], a singular integral equation method was developed, where a careful choice of the expanding functions for E_x and E_y is devised to make more accurate the well-known Galerkin's procedure for numerical solution. Several numerical methods, such as the finite-integration method [5], the finite-element method [6], [7], and the boundary-element method [8], [9], have been developed to solve waveguide discontinuity problems, and they are appropriate for investigating structures of complicating shape, where the em-field distribution cannot be described in a closed form; therefore, practical impossibility of analytical solutions is evident. Among the methods that do not preclude analytical solutions, the mode-matching method [10]–[14] is the most convenient and widely used one, although its applicability is restricted in certain geometrical configurations, where the em-field can be represented either by an infinite set of modes or by an integral transform. References [10]–[14] indeed treat geometries similar to dc breaks, but with some simplifications (there is no dielectric, the terminations of the open junction are added *ad hoc*, or the output waveguide is ignored); in this literature, the field-continuity equations are satisfied at each boundary of the discontinuity and an infinite set of linear algebraic equations for the field expansion coefficients is obtained, which is subsequently truncated and numerically solved.

Our objective in this paper is to derive analytical expressions for the scattering coefficients of a flanged rectangular waveguide open junction, used in a dc break, with dielectric loading of the gap space (see Fig. 1). The dielectric sleeve helps to avoid sparks in the component because of the applied high dc voltage. The method used is the mode-matching with appropriate field expansion in Fourier series and integrals. A similar problem of a circumferential gap in a circular waveguide has been studied in the monomode [15], as well as the multimode [16] waveguide case. In these papers, the incident wave is the circular symmetric TE_{01} with no longitudinal currents on the waveguide wall. The transverse currents do not considerably charge the boundary of the gap and thus little energy is radiated into the surrounding space. In the case of a rectangular gap, charged by the dominant TE_{10} mode, the image is completely different and considerable radiation is expected through the gap.

This paper is organized as follows. In Section II we describe our two-dimensional (2-D) model, the basic equations, and the field representation used in the analysis. In Section III the mathematical formulation is presented for the analytic computation of the scattering coefficients. In Section IV the same formulation is applied to the field generated by the dielectric interface. Results of the analytic solution are presented in Section V and compared with two numerical codes, along with a discussion for the reliability of the analysis in different domains of gap width and dielectric loading.

Manuscript received December 10, 1993; revised October 18, 1996. The work of C. T. Iatrou was supported by the European Union program "Human Capital and Mobility" under Contract ERBCHBGCT920207.

C. T. Iatrou was with the Laboratori Nazionali di Legnaro, Istituto Nazionale di Fisica Nucleare, Legnaro (PD), I-35020, Italy. He is now with Forschungszentrum Karlsruhe, Institut für Technische Physik, Karlsruhe, D-76021, Germany.

M. Cavenago is with the Laboratori Nazionali di Legnaro, Istituto Nazionale di Fisica Nucleare, Legnaro (PD), I-35020, Italy.

Publisher Item Identifier S 0018-9480(97)00819-3.

0018–9480/97$10.00 © 1997 IEEE

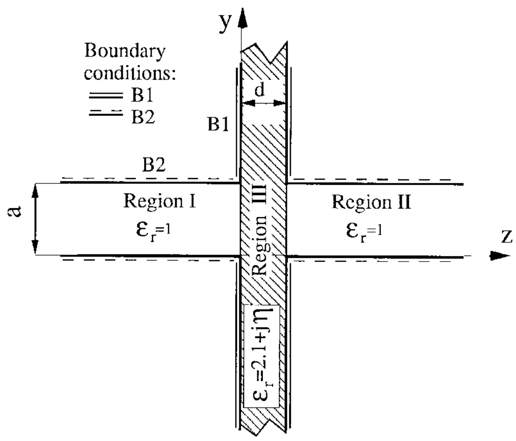

Fig. 1. The infinite parallel-planes waveguide model of the dc break: zy cross section of the model and the metallic boundaries.

II. Model and Basic Equations

A 2-D model for a rectangular waveguide open junction with transverse dimensions $(a \times b)$ consists of two, normally intersected, infinite parallel-planes waveguides, as shown in Fig. 1. The parallel planes of the horizontal waveguide are infinitely extended in the x- and z-directions, while the distance between them is taken equal to the small transverse dimension a of the actual rectangular waveguide. As for the vertical waveguide, which is assumed to be filled with dielectric material of relative permittivity ϵ_r, the parallel planes are extended to infinity in the x- and y-directions, while the distance between them is denoted by d and represents the width of the open junction.

The wave energy incident from $z = -\infty$ on the open junction is partially reflected and partially transmitted. Some of the energy is coupled to the vertical dielectric waveguide. Since no free current is present, $\nabla \cdot \boldsymbol{D} = 0$ from which

$$\boldsymbol{D} = -\nabla \times \boldsymbol{F}$$

where $\boldsymbol{F}$ is an electric vector potential, also called the magnetic Herztian potential [17] or the antipotential; moreover, since the incident TE_{10} dominant mode of a monomode waveguide has no y-magnetic component, we assume that the electric potential $\boldsymbol{F}$ has no y-component. An appropriate choice for the electric potential is then

$$\boldsymbol{F} = \epsilon_0[X(x,y,z)\boldsymbol{e}_x - \epsilon_r Z(x,y,z)\boldsymbol{e}_z] \quad (1)$$

where $X(x,y,z)$ and $Z(x,y,z)$ have dimensions of potential.

The fields $\boldsymbol{E}$ and $\boldsymbol{H}$ in terms of $\boldsymbol{F}$ are given by [17]

$$\boldsymbol{E} = -\frac{1}{\epsilon}\nabla \times \boldsymbol{F} \quad (2)$$

$$\boldsymbol{H} = j\frac{1}{\omega\mu}\nabla \times \frac{\nabla}{\epsilon} \times \boldsymbol{F} \quad (3)$$

where the dielectric permittivity $\epsilon = \epsilon_0\epsilon_r(z)$ is in general function of z. The electric potential $\boldsymbol{F}$ satisfies the wave equation $\Delta\boldsymbol{F} + \epsilon\mu\omega^2\boldsymbol{F} = 0$ in uniform media.

Applying boundary conditions for the tangential components of $\boldsymbol{E}$ and the normal components of $\boldsymbol{H}$ we obtain the following boundary conditions for the components X and Z on the metallic boundary B_1 (see Fig. 1)

$$Z = 0 \quad (4a)$$

$$\frac{1}{\epsilon_r}\partial_z X = 0 \quad (4b)$$

and on the metallic boundary B_2

$$\partial_y Z = 0 \quad (5a)$$

$$\frac{1}{\epsilon_r}\partial_y X = 0 \quad (5b)$$

where ∂_v denotes partial derivative with respect to variable v.

On the interface between the two media the normal components of $\boldsymbol{D}$ and $\boldsymbol{H}$ and the tangential components of $\boldsymbol{E}$ and $\boldsymbol{H}$ must be continuous. So, using the notation "$f = \text{cont}$" to mean that $f(z)$ is continuous on the air-dielectric interface, we write the following four linearly independent interface conditions for the potential functions X and Z

$$X = \text{cont} \quad (6a)$$

$$\frac{1}{\epsilon_r}\partial_z X = \text{cont} \quad (6b)$$

$$Z = \text{cont} \quad (6c)$$

$$\partial_z Z - \frac{1}{\epsilon_r}\partial_x X = \text{cont}. \quad (6d)$$

Note that the X potential component is separated satisfying conditions (6a) and (6b); our choice of using electric potential therefore gives only one interface equation that couples X and Z out of four. If we had chosen H_x and E_x we would have two coupling conditions; if we had chosen H_z and E_z (corresponding to the TE and TM modes of the incoming waveguide) we would have four coupling conditions.

Let us now represent the potential functions X and Z in Regions I and II (see Fig. 1) as infinite sums on Fourier components

$$\begin{bmatrix} X_{\text{I}} \\ Z_{\text{I}} \end{bmatrix} = e^{ikz}e^{jk_x x}\begin{bmatrix} 1 \\ 0 \end{bmatrix} + \sum_{m=0}^{\infty}\begin{bmatrix} a_{m_X} \\ a_{m_Z} \end{bmatrix}\cos(k_{ym}y)e^{k_{zm}z}e^{jk_x x} \quad (7a)$$

$$\begin{bmatrix} X_{\text{II}} \\ Z_{\text{II}} \end{bmatrix} = \sum_{m=0}^{\infty}\begin{bmatrix} b_{m_X} \\ b_{m_Z} \end{bmatrix}\cos(k_{ym}y)e^{-k_{zm}(z-d)}e^{jk_x x} \quad (7b)$$

where $k_x = \pi/b$ and $k_{ym} = m\pi/a$ are the guiding wavenumbers in the x- and y-direction, respectively, $k = (\omega^2/c^2 - k_x^2)^{1/2}$ is the guided wavenumber for the propagating TE_{10} mode, $k_{zm} = (k_{ym}^2 - k^2)^{1/2}$ are the attenuation constants for evanescent modes for $m \geqslant 1$, and $k_{z0} = -jk$. Note that the incoming TE_{10} mode is produced by the only driving term, which appears in the X potential component. The coefficients a_{m_X} and a_{m_Z} correspond to reflected waves, back to Region I, while b_{m_X} and b_{m_Z} correspond to transmitted waves, through the open junction to Region II.

The fact that the potential function Z does not contain any driving term, combined with the interface condition $(6d)$, implies that this potential component and the corresponding waves are generated just because of the presence of the dielectric discontinuity at $z = 0$ and $z = d$ and not because of the geometric gap. Otherwise, if there were no dielectric in the vertical waveguide, the quantity $(1/\epsilon_r)\partial_x X$ would be continuous, so that $\partial_z Z$ and Z itself would be continuous at the interface; therefore, Z would satisfy the equations of a damped resonator without internal discontinuities in the union of Regions I, II, and III, with mixed boundary condition $(= 0)$; this would imply $Z = 0$.

In Region III we represent the functions Z and X as Fourier integrals

$$\begin{bmatrix} X_{\mathrm{III}} \\ Z_{\mathrm{III}} \end{bmatrix} = \int_{-\infty}^{+\infty} \frac{dk_y}{2\pi} e^{-jk_y y} \cdot \left(\begin{bmatrix} c_X \\ c_Z \end{bmatrix} e^{jk_z z} + \begin{bmatrix} d_X \\ d_Z \end{bmatrix} e^{-jk_z z} \right) e^{jk_x x} \tag{8}$$

where $k_z = (k'^2 - k_y^2)^{1/2}$ and $k' = (\epsilon_r \omega^2/c^2 - k_x^2)^{1/2}$, with the square root analytically continued for nonpositive arguments (the complex plane cut is yet to be defined, but it will be shown that the results do not depend on its particular choice). Note that the coefficients c_X, d_X, c_Z, and d_Z are functions of k_y.

From (7) the propagating field in Regions I and II can be computed. The reflection s_{11} and transmission s_{21} scattering coefficients in power are then given, in terms of the Fourier potential coefficients, by the following formulas:

$$s_{11} = \left(a_{0X} - \frac{k_x}{k} a_{0Z} \right) \left(a_{0X}^* - \frac{k_x}{k} a_{0Z}^* \right) \tag{9a}$$

$$s_{21} = \left(b_{0X} - \frac{k_x}{k} b_{0Z} \right) \left(b_{0X}^* - \frac{k_x}{k} b_{0Z}^* \right) \tag{9b}$$

where the superscript * denotes complex conjugate quantities.

III. Matrix Equations and Solution for the X Potential

Application of the condition (6a) at $z = 0$ and $z = d$, multiplication by $\cos(k_{yn} y')$ and integration on y' from $y' = 0$ to $y' = a$ yields

$$\gamma_n \begin{bmatrix} \delta_{n0} + a_{nX} \\ b_{nX} \end{bmatrix} = \int_{-\infty}^{+\infty} \frac{dk_y}{2\pi} f_n(-k_y) \cdot \begin{bmatrix} 1 & 1 \\ e^{jk_z d} & e^{-jk_z d} \end{bmatrix} \begin{bmatrix} c_X \\ d_X \end{bmatrix} \tag{10}$$

where $\gamma_n = (1 + \delta_{n0})/2$ is a numerical factor, and the function f_n expresses coupling between discrete modes and the continuous k_y, defined as

$$f_n(\alpha) = \frac{1}{a} \int_0^a dy e^{j\alpha y} \cos(k_{yn} y).$$

The second interface condition $(6b)$ for the X-potential function is then applied at $z = 0$ and $z = d$, multiplied by $e^{jk'_y y}$ and integrated on y from $y = -\infty$ to $y = +\infty$, to yield

$$a\epsilon_r \sum_{m=0}^{\infty} k_{zm} f_m(k_y) \begin{bmatrix} -\delta_{m0} + a_{mX} \\ b_{mX} \end{bmatrix} = \begin{bmatrix} 1 & -1 \\ e^{jk_z d} & -e^{-jk_z d} \end{bmatrix} \begin{bmatrix} c_X \\ d_X \end{bmatrix}. \tag{11}$$

With simple matrix manipulations, (11) can be solved for c_X and d_X and the result is introduced to (10) to yield the following system for the X-function coefficients:

$$\sum_{m=0}^{\infty} k_{zm} \begin{bmatrix} I_{nm} + \beta_{nm} & J_{nm} \\ J_{mn} & I_{nm} + \beta_{nm} \end{bmatrix} \begin{bmatrix} a_{mX} \\ b_{mX} \end{bmatrix} = - \begin{bmatrix} \frac{a}{\epsilon_r} \delta_{n0} + jkI_{n0} \\ 2jkJ_{n0} \end{bmatrix} \tag{12}$$

where $\beta_{nm} = a\gamma_n \delta_{nm}/\epsilon_r k_{zn}$ is a purely diagonal term and

$$\begin{bmatrix} I_{nm} \\ J_{nm} \end{bmatrix} = -a^2 d \int_{-\infty}^{+\infty} \frac{dk_y}{2\pi} f_n(-k_y) f_m(k_y) \frac{1}{k_z d} \cdot \begin{bmatrix} \cot(k_z d) \\ \csc(k_z d) \end{bmatrix}. \tag{13}$$

The integrands in (13) are even in k_z, so that only the square of k_z and not k_z itself appears in any series expansion of the integrand; this makes immaterial the choice of cut in the k_y complex plane. Moreover, both integrals in (13) have infinite poles in the complex plane. A pair of poles is on the real axis, at $k_y = \pm k'$, corresponding to the dominant TE_{10} mode, which always propagates in the dielectric waveguide. An infinite pair of poles are at $k_y = \pm jk_\ell$, where $k_\ell = (\ell^2\pi^2/d^2 - k'^2)^{1/2}$ and correspond to $TE_{1\ell}$ and $TM_{1\ell}$ modes, which may be propagating or evanescent, depending on the width d of the dielectric waveguide. For small values of d, these modes are evanescent and the poles are on the imaginary axis. Each of these modes start to propagate as d becomes greater than $\ell\pi/k'$.

Let us discuss the meaning of results (unphysical) if singularities in the integrand were fixed by the principal value. The I_{nm} and J_{nm} found were real. The structure of (12) and the real values of I_{nm} and J_{nm} always impose a solution satisfying the relation $|s_{11}| + |s_{21}| = 1$, which means that there is no power radiated into the dielectric waveguide, whatever the value of d. A way to interpret this result is to consider that there are, indeed, waves propagating into the dielectric waveguide, but these waves are reflected back from the boundaries at $y = \pm\infty$ since no boundary conditions correspondent to purely outgoing waves were imposed there. A simple way to avoid this effect is to introduce a small damping on the waves that travel along the dielectric waveguide, so that no power reaches the boundaries at $y = \pm\infty$ to be reflected back. In mathematical terms, when evaluating the integrals on k_y in (13) by the residue method, we add an imaginary part $\eta > 0$ to the relative dielectric constant $(\epsilon_r \to \epsilon_r + j\eta)$. In the complex plane, the pair of previously real poles at $k_y = \pm k'$ is now moved from the real axis, taking an imaginary part proportional to η. Likewise, the infinite pairs of the previously imaginary poles (for small d), are now displaced for a real part proportional to η. The method is analogous to "Landau prescription" for the choice of the integration path in instability studies. In the limit of vanishing η, the following expressions for the integrals in (13) are obtained: if $(-1)^n = -(-1)^m$ then $I_{nm} = J_{nm} = 0$, and if $(-1)^n = (-1)^m$ then see (14), shown at the bottom of the next page, where the following notations are used: $s' = k'a/\pi, s_\ell = k_\ell a/\pi$, and

$$\begin{bmatrix} g'_n \\ g_{n\ell} \end{bmatrix} = \frac{a^3}{2\pi d^2} \begin{bmatrix} -(s'^2 - n^2)^{-1} \\ 2(s_\ell^2 + n^2)^{-1} \end{bmatrix} \tag{15a}$$

$$\begin{bmatrix} c' \\ c_\ell \end{bmatrix} = \frac{a^3}{d\pi^3} \begin{bmatrix} js'(1 - e^{j\pi s'}) \\ 2s_\ell(1 - e^{-\pi s_\ell}) \end{bmatrix}. \tag{15b}$$

In the above expressions primed quantities refer to the $\pm k'$ poles while these with subscript ℓ to the first of the k_ℓ poles. For small values of d the main contribution to the integrals comes from the k' poles, that means the propagating waves in the dielectric waveguide, while the significance of the evanescent waves, represented by the k_ℓ poles, is increasing with d.

Assuming that $d \ll \pi/k'$, it is sufficient to keep only the first $(\ell = 1)$ term of the infinite sum in (14).

After substituting (14) into (12), we note that the a_{n_X} and b_{n_X} vanish for n odd, and the following system is obtained for the even order coefficients of the X potential component

$$\begin{bmatrix} D_{1n} & D_{2n} \\ D_{2n} & D_{1n} \end{bmatrix} \begin{bmatrix} a_{n_X} \\ b_{n_X} \end{bmatrix} = -\begin{bmatrix} \dfrac{Q'}{s'^2 - n^2} - \dfrac{Q_1}{s_1^2 + m^2} - e_n \\ \dfrac{Q'}{s'^2 - n^2} + \dfrac{Q_1}{s_1^2 + m^2} - f_n \end{bmatrix} \tag{16}$$

where

$$\begin{bmatrix} D_{1n} \\ D_{2n} \end{bmatrix} = \frac{1}{2\epsilon_r} \begin{bmatrix} \gamma_n \\ 0 \end{bmatrix} + \frac{k_{zn}}{a} \begin{bmatrix} g'_n + g_{n1} \\ g'_n - g_{n1} \end{bmatrix} \tag{17a}$$

$$\begin{aligned} \begin{bmatrix} e_n \\ f_n \end{bmatrix} &= \begin{bmatrix} \dfrac{\gamma_n}{\epsilon_r} + j\dfrac{k}{a}(g'_n + g_{n1}\delta_{n0} \\ j\dfrac{k}{a}(g'_n - g_{n1})\delta_{n0} \end{bmatrix} \\ &\quad + j\frac{k}{a} \begin{bmatrix} \dfrac{c'}{s'^2(s'^2 - n^2)} - \dfrac{c_1}{s_1^2(s_1^2 - n^2)} \\ \dfrac{c'}{s'^2(s'^2 - n^2)} + \dfrac{c_1}{s_1^2(s_1^2 - n^2)} \end{bmatrix} \end{aligned} \tag{17b}$$

and we introduce the collective variables

$$\begin{bmatrix} Q' \\ Q_1 \end{bmatrix} = \frac{1}{a} \sum_{m=0}^{\infty} k_{zm} \begin{bmatrix} c'(a_{m_X} + b_{m_X})(s'^2 - m^2)^{-1} \\ c_1(a_{m_X} - b_{m_X})(s_1^2 + m^2)^{-1} \end{bmatrix}. \tag{18}$$

The infinite system (16) and (18) can be solved. Indeed, from (16) we obtain expressions for the coefficients a_{n_X} and b_{n_X} in terms of Q' and Q_1

$$\begin{aligned} \begin{bmatrix} a_{n_X} \\ b_{n_X} \end{bmatrix} &= -\frac{1}{D_n} \begin{bmatrix} D_{1n} & -D_{2n} \\ -D_{2n} & D_{1n} \end{bmatrix} \\ &\quad \cdot \begin{bmatrix} \dfrac{Q'}{s'^2 - n^2} - \dfrac{Q_1}{s_1^2 + m^2} - e_n \\ \dfrac{Q'}{s'^2 - n^2} + \dfrac{Q_1}{s_1^2 + m^2} - f_n \end{bmatrix} \end{aligned} \tag{19}$$

where $D_n = D_{1n}^2 - D_{2n}^2$. Introducing (19) into (18) we get a 2×2 system for unknowns Q' and Q_1, which is then solved to give

$$Q' = \frac{F_1 + F_2}{1 + 2F} \tag{20a}$$

and

$$Q_1 = \frac{G_1 + G_2}{1 - 2G} \tag{20b}$$

where

$$\begin{bmatrix} F_1 \\ F_2 \end{bmatrix} = -\frac{c'}{a} \sum_{m=0}^{\infty} \frac{k_{zm}}{s'^2 - m^2} \frac{1}{D_m} \begin{bmatrix} D_{1m} & -D_{2m} \\ -D_{2m} & D_{1m} \end{bmatrix} \begin{bmatrix} e_n \\ f_n \end{bmatrix} \tag{21a}$$

$$\begin{bmatrix} G_1 \\ G_2 \end{bmatrix} = -\frac{c_1}{a} \sum_{m=0}^{\infty} \frac{k_{zm}}{s_1^2 + m^2} \frac{1}{D_m} \begin{bmatrix} D_{1m} & -D_{2m} \\ -D_{2m} & D_{1m} \end{bmatrix} \begin{bmatrix} e_n \\ f_n \end{bmatrix} \tag{21b}$$

$$F = \frac{c'}{a} \sum_{m=0}^{\infty} \frac{k_{zm}}{(s'^2 - m^2)^2} \frac{D_{1m} - D_{2m}}{D_m} \tag{21c}$$

$$G = \frac{c_1}{a} \sum_{m=0}^{\infty} \frac{k_{zm}}{(s_1^2 + m^2)^2} \frac{D_{1m} + D_{2m}}{D_m} \tag{21d}$$

and $D_m = D_{1m}^2 - D_{2m}^2$. Substituting (20) back to (19) and applying this equation for $n = 0$, analytical expressions for potential coefficients a_{0_X} and b_{0_X} are trivially obtained.

IV. The Coefficient of Z

Combining (4a) and (6c) we note that the Z function satisfies for every y the equations

$$Z_{\mathrm{I}}(x, y, 0) I(y) = Z_{\mathrm{III}}(x, y, 0) \tag{22a}$$

$$Z_{\mathrm{II}}(x, y, d) I(y) = Z_{\mathrm{III}}(x, y, d) \tag{22b}$$

(where $I(y) = 1$ for $0 \leq y \leq a$ and is zero elsewhere); their solution will be similar, but not equal to the solution for the X function Fourier coefficients.

After substituting the expression for fields (7) and (8), we Fourier transform (22) obtaining for each k_y

$$\begin{bmatrix} 1 & 1 \\ e^{jk_z d} & e^{-jk_z d} \end{bmatrix} \begin{bmatrix} c_Z \\ d_Z \end{bmatrix} = a \sum_{m=0}^{\infty} f_m(k_y) \begin{bmatrix} a_{m_Z} \\ b_{m_Z} \end{bmatrix} \tag{23}$$

where not only c_Z and d_Z, but also k_z depend on k_y. The remaining condition (6d) applied to the two interfaces at $z = 0$ and $z = d$ gives the two equations

$$\begin{aligned} &\sum_{m=0} \left(k_{zm} \begin{bmatrix} a_{m_Z} \\ b_{m_Z} \end{bmatrix} - jk_b\epsilon_d \begin{bmatrix} \delta_{m,0} + a_{m_X} \\ -b_{m_X} \end{bmatrix} \right) \cos\frac{\pi m y}{a} \\ &\quad = \int \frac{\mathrm{d}k_y}{2\pi} \times e^{-jk_y y} jk_z \begin{bmatrix} 1 & -1 \\ -e^{jk_z d} & e^{-jk_z d} \end{bmatrix} \begin{bmatrix} c_Z \\ d_Z \end{bmatrix} \end{aligned} \tag{24}$$

$$\begin{bmatrix} I_{nm} \\ J_{nm} \end{bmatrix} = \begin{bmatrix} g'_n \\ g'_n \end{bmatrix} \delta_{nm} + \sum_{\ell=1}^{\infty} \begin{bmatrix} g_{n\ell}\delta_{nm} + \dfrac{c'}{(s'^2 - n^2)(s'^2 - m^2)} + \dfrac{(-1)^\ell c_\ell}{(s_\ell^2 + n^2)(s_\ell^2 + m^2)} \Bigg) \\ -g_{n\ell}\delta_{nm} + \dfrac{c'}{(s'^2 - n^2)(s'^2 - m^2)} + \dfrac{-(-1)^\ell c_\ell}{(s_\ell^2 + n^2)(s_\ell^2 + m^2)} \Bigg) \end{bmatrix} \tag{14}$$

where we expressed Z in terms of a_{mZ}, b_{mZ}, c_Z, and d_Z and X similarly, thanks to (7) and (8). Here the quantity $\epsilon_d \equiv 1 - \epsilon_r^{-1}$ comes from the jump of dieletric constant at interface; it is positive for ordinary dieletric.

Equation (24) holds only for $0 \leq y \leq a$; for any given m, let $\boldsymbol{u}_m$ indicate the expression in round brackets of (24); $\boldsymbol{u}_m$ are two-component vectors and are just useful shorthand, since they do not depend on y. In the right-hand side (RHS) of (24), c_Z may be easily expressed in terms of a_{mZ} thanks to (23); we note that unfortunately, when $y = 0$ or $y = a$ the integration on $\mathrm{d}ky$ is divergent for $k_y \to \infty$ due to the jk_z factor. By the naive approach of multiplying (24) with $\cos(\pi m y/a)$ and integrating from 0 to a we could obtain directly expressions for $\boldsymbol{u}_m$ in term of a_{mZ}, still plagued by divergent integrals, which makes residue method inapplicable. To avoid this, we follow a more tortuous path, which practically gives the same results (35).

We first define the integrals of the eigenmodes

$$e_m(y) = \int_{a/2}^{y} \cos(\pi m y/a) \tag{25}$$

and, correspondingly, we integrate (24) from $a/2$ to y

$$\sum_{m=0} \boldsymbol{u}_m e_m(y) = a \int \frac{\mathrm{d}ky}{2\pi} k_z \frac{e^{-ik_y a/2} - e^{-ik_y y}}{k_y} \cdot \sum_{m=0} f_m(k_y) \begin{bmatrix} -c_{hyp} & s_{hyp} \\ s_{hyp} & -c_{hyp} \end{bmatrix} \begin{bmatrix} a_{mZ} \\ b_{mZ} \end{bmatrix} \tag{26}$$

where the quantities $c_{hyp} = 1/\tanh(jk_z d)$ and $s_{hyp} = 1/\sinh(jk_z d)$, which came from matrix inversion in (23) and product in (24), still depend on k_y. Note that integrating on y cancels singularity for $k_y \to \infty$, but e_m are no longer orthogonal.

We can now multiply (26) by $a^{-1}\sin(\pi n y/a)$ and integrate from 0 to a, obtaining (after performing the straightforward integrations implied in e_m and $f(k_y, m)$, the simplifications of k_y factors and exploiting symmetry about $y = a/2$)

$$\frac{a}{2\pi n}\boldsymbol{u}_n - \frac{a}{\pi n}\boldsymbol{u}_0 = a^2 \sum_{m \text{ even}} \begin{bmatrix} -L_{nm} & M_{nm} \\ M_{mn} & -L_{mn} \end{bmatrix} \begin{bmatrix} a_{mZ} \\ b_{mZ} \end{bmatrix} \tag{27}$$

valid for $n \neq 0$, where L and M, computing $\mathrm{d}ky$ integration by residue method and the elementary $\mathrm{d}y$ integrations, have similar expressions

$$\pi n a M_{nm} = -\delta_{m0}\frac{q_0}{\sinh(q_0 d)} + \frac{q_m \delta_{nm} T_m}{2\sinh(q_m d)} - \sum_{l=1} \frac{n^2}{s_\ell^2 + n^2}\,\frac{j^{2\ell} c_\ell^Z}{s_\ell^2 + m^2} \tag{28}$$

with $T_0 = 0$ and $T_m = 1$ otherwise; here $q_m = (m^2\pi^2/a^2 - k'^2)^{1/2}$ and the pole strength is given by

$$c_\ell^Z = 2\frac{a^2\ell^2}{\pi d^3 s_\ell}[1 - \exp(-k_\ell a)].$$

The expression for L corresponding to (28) has $j^{2\ell}$ deleted and $\sinh$ replaced by $\tanh$.

We recognize that first and second term of (28) inserted in (27) can be merged with $\boldsymbol{u}_0$ and $\boldsymbol{u}_n$ after defining for any n a new vector

$$\boldsymbol{v}_n \equiv \boldsymbol{u}_n + q_n \begin{bmatrix} 1/\tanh(q_n d) & -1/\sinh(q_n d) \\ -1/\sinh(q_n d) & 1/\tanh(q_n d) \end{bmatrix} \begin{bmatrix} a_{mZ} \\ b_{mZ} \end{bmatrix}. \tag{29}$$

Furthermore, by defining

$$E_{1_n} = \gamma_n(k_n^z + q_n/\tanh(q_n d))$$
$$E_{2_n} = -\gamma_n q_n/\sinh(q_n d))$$

(29) becomes

$$\boldsymbol{v}_n = \frac{1}{\gamma_n}\begin{bmatrix} E_{1_n} & E_{2_n} \\ E_{2_n} & E_{1_n} \end{bmatrix} \begin{bmatrix} a_Z \\ b_{nZ} \end{bmatrix} - jk_b\epsilon_d \begin{bmatrix} \delta_{m,0} + a_{mX} \\ -b_{mX} \end{bmatrix}. \tag{30}$$

With this notation, (27) becomes

$$\gamma_n \boldsymbol{v}_n - \boldsymbol{v}_0 = \sum_{\ell=1}\sum_{m=0} \frac{n^2}{s_\ell^2 + n^2}\,\frac{c_\ell^Z}{s_\ell^2 + m^2} \cdot \begin{bmatrix} 1 & -j^{2\ell} \\ -j^{2\ell} & 1 \end{bmatrix} \begin{bmatrix} a_{mZ} \\ b_{mZ} \end{bmatrix}. \tag{31}$$

It is convenient to distribute (31) into parts, using the identity

$$\frac{n^2}{n^2 + s_\ell^2}\,\frac{1}{m^2 + s_\ell^2} = -\frac{1}{n^2 + s_\ell^2} + \frac{1}{m^2 + s_\ell^2} + \frac{1}{n^2 + s_\ell^2}\,\frac{m^2}{m^2 + s_\ell^2}. \tag{32}$$

Some direct information from boundary condition makes (31) simpler to be solved. From (22) taken at $y = 0, z = 0$ or $z = d$ we know that

$$\sum_m a_{mZ} = \sum_m b_{mZ} = 0.$$

This conclusion is corroborated by the fact that otherwise (31) would contain a divergent part, precisely that arising from first term of RHS of (32). This part is instead zero because of $\Sigma_m\ a_{mZ} = \Sigma_m\ b_{mZ} = 0$. Second, since we search a finite solution for Z and X, we can assume that sums of $a_{mX}, a_{mZ}, b_{mX}, b_{mZ}$ are convergent, which implies $m a_{mZ} \to 0$ when $m \to \infty$. From expression (30), knowing that $E_{1_n} \propto n$ and E_{2_n} is exponentially decreasing with n, we conclude that

$$\lim_{n\to\infty} \boldsymbol{v}_n = 0. \tag{33}$$

Taking the limit of (31) for $n \to \infty$ and observing that the part arising from the third term of (32) converges to zero, we are left with the second part only

$$\boldsymbol{v}_0 = -\sum_{l=1}\sum_{m=0} \frac{c_\ell^Z}{s_\ell^2 + m^2} \begin{bmatrix} 1 & -j^{2\ell} \\ -j^{2\ell} & 1 \end{bmatrix} \begin{bmatrix} a_{mZ} \\ b_{mZ} \end{bmatrix}. \tag{34}$$

Adding (34) to (31), we get

$$\gamma_n \boldsymbol{v}_n = +\sum_{l=1} \frac{c_\ell^Z}{s_\ell^2 + n^2} \sum_{m=0} \frac{m^2}{s_\ell^2 + m^2} \begin{bmatrix} 1 & -j^{2\ell} \\ -j^{2\ell} & 1 \end{bmatrix} \begin{bmatrix} a_{mZ} \\ b_{mZ} \end{bmatrix} \tag{35}$$

for any given even $n \neq 0$. As to $\boldsymbol{v}_0$, we note that (34) becomes of the form (35) by substituting $1/(s_\ell^2 + m^2)$ with $s_\ell^{-2}(1 - m^2/(s_\ell^2 + m^2))$; thus (35) applies to every even $n \geq 0$.

We now define the collective variable

$$C_1 = -\sum_{m=0} \frac{a_{m_Z} + b_{m_Z}}{m^2 + s_1^2} \tag{36}$$

which is a sort of projection on a privileged axis of $\{a_{m_Z}, b_{m_Z}\}$ space. Consistently to the approximation done for X, we truncate the RHS of (35) to the first term in ℓ, so that (35) may be solved as

$$\begin{bmatrix} a_{n_Z} \\ b_{n_Z} \end{bmatrix} = \begin{bmatrix} E_{1_n} & E_{2_n} \\ E_{2_n} & E_{1_n} \end{bmatrix}^{-1} \left(jk_b\epsilon_d \begin{bmatrix} \delta_{n,0} + a_{n_X} \\ -b_{n_X} \end{bmatrix} - \frac{c_1^Z C_1}{n^2 + s_1^2} \begin{bmatrix} 1 \\ 1 \end{bmatrix} \right). \tag{37}$$

By substituting (37) into (36), we find a linear equation for the collective variable, of the form $C_1 = F_Z - c_1^Z H_Z C_1$, with the coefficients

$$F_Z = -\sum_n \frac{n^2}{n^2 + s_1^2} \frac{jk_b\epsilon_d\gamma_n(\delta_{n0} + a_{n_X} - b_{n_X})}{E_{1_n} + E_{2_n}} \tag{38}$$

$$H_Z = -\sum_n \frac{2n^2}{(n^2 + s_1^2)^2(E_{1_n} + E_{2_n})}. \tag{39}$$

The value of the collective variable is thus

$$C_1 = \frac{F_Z}{1 + c_1^Z H_Z}. \tag{40}$$

This equation together with (37) are the complete solution for $Z; n = 0$ case is trivial.

Let us mention how the symmetries of the model geometry (reflection about $y = a/2$ and reflection about $z = d/2$) has entered in the final result. The odd components (respect to y-reflection) are the m odd components, which are not excited and they had been found to be zero. Both symmetric and antisymmetric components (respect to the z reflection) are excited by the transmitter; indeed we found collective variables which are symmetric (namely, Q' and C_1, that are proportional to $a + b$ where a and b are a_{m_X} and b_{m_X} or a_{m_Z} and b_{m_Z} as appropriate) and others which are antisymmetric (namely, Q_1 proportional to $a - b$).

V. Comparison with Numerical Results

In this section, we show comparisons of results of our analytic theory to numerical results obtained from two codes. One is the well-known Maxwell's equations using finite integration algorithm (MAFIA) [5] and the other, provisionally called microwave problem (MP), is being developed by Cavenago. The results from these codes are generally in agreement. Results from MP are preliminary; since it is a 2-D code (using ten mesh nodes to model the gap) it runs very fast (one minute per simulation) and 2-D parameter studies are well possible.

To simplify comparison, we consider only the gap thickness d and the dieletric index ϵ_r as variable parameters; other data applies to WR-62 (alias WG-18, alias R140) rectangular waveguides, operating at 14.4 GHz. The waveguide transverse

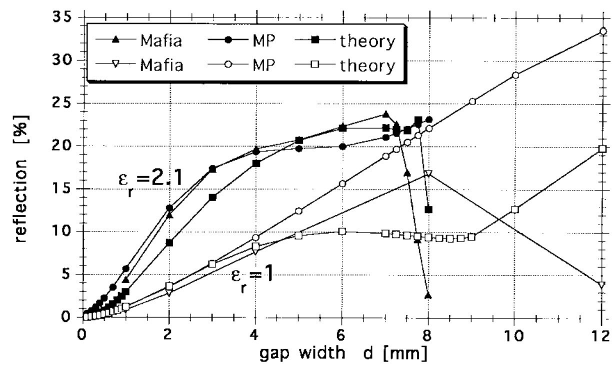

Fig. 2. The reflection coefficient s_{11} (in %) as a function of d, for $\epsilon_r = 1$ (empty markers) and 2.1 (filled markers). Analytical result are compared with result from two numerical codes.

dimensions are: $a = 7.9$ mm, and $b = 15.8$ mm. In practical application d is typically 1 mm, so here d will range from 0.1 mm to about 10 mm; the cases $\epsilon_r = 1$ (air gap) and $\epsilon_r = 2.1$ (Teflon) are particularly important.

From numerical code MP, transmission, reflection, and radiation can be directly found; their sum is of course unity within the precision of the code; we plot unnormalized results. In the case of MAFIA results, it was convenient to obtain transmission and reflection directly and to compute radiation as difference from unity. From the present analytical theory transmission and reflection are directly obtained; radiation is obtained by difference, which may lead to larger relative errors. In Figs. 2–4 we plot transmission and reflection for $\epsilon_r = 1$ and 2.1. We first note that analytical theory assumes that k_1 is real, which implies

$$d < \pi/k' = \pi[\epsilon_r(\omega/c)^2 - (\pi/b)^2]^{-1/2} \equiv d_m(\epsilon_r)$$

that is $d_m = 13.6$ mm for $\epsilon_r = 1$ and $d_m \cong 8$ mm for $\epsilon_r = 2.1$. In the first case, remarkable also because the X function only affects results, the agreement of MP and analytical theory is rather good for transmission and radiation for $d < d_1 = 8$ mm. The oscillation for $d > d_1$ of the analytical results is explained by the fact that k_1 becomes imaginary when d exceeds d_m; we conclude that the results are reliable for $d < 0.5d_m$, where 0.5 is a conservative safety factor; that leads to the criterion

$$d < 0.5 \frac{\pi}{\sqrt{\epsilon_r \frac{\omega^2}{c^2} - \frac{\pi^2}{b^2}}} \tag{41}$$

for every ϵ_r. For $\epsilon_r = 2.1$ we indeed find that the analytical result (including reflection) are reliable up to $d < d_2 = 5$ mm, in agreement with criterion (41).

In Fig. 5 we plot reflection, radiation, and transmission for $d = 1$ mm (analytical result for radiation have a large relative error). From criterion (41) we expect that reliable results will be obtained for $\epsilon_r < \epsilon_1 \equiv (\pi c/\omega)^2(b^{-2} + 0.25d^{-2})$; that is $\epsilon_1 \cong 27$ for $d = 1$ mm. We note that the analytically calculated transmission is indeed in good agreement with the numerical results. As for reflection, agreement is generally rather good, with some large error close to $\epsilon_r < \epsilon_2 \cong 7$, that can be related to the fact that q_2 vanishes and then becomes imaginary when ϵ_r reaches and exceeds $\epsilon_3 = (\pi c/\omega)^2(b^{-2} + 4a^{-2}) = 7.38$.

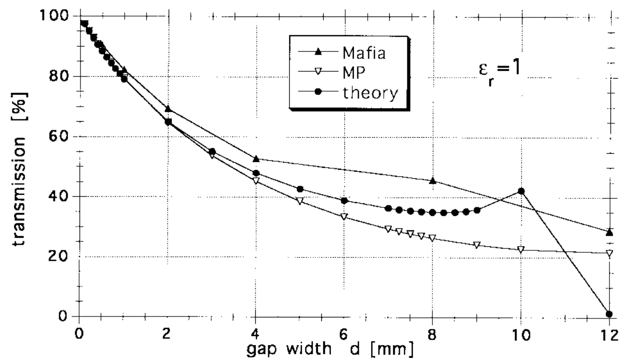

Fig. 3. The transmission coefficient s_{21} (in %) as a function of d, for $\epsilon_r = 1$.

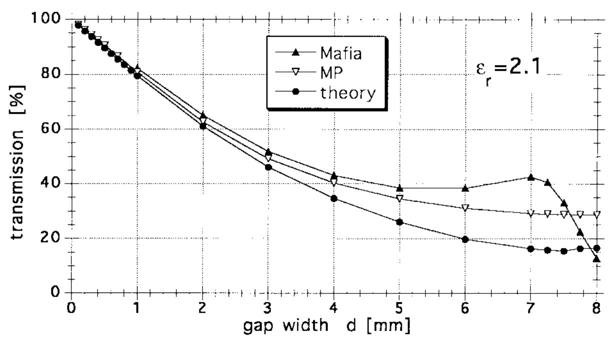

Fig. 4. The transmission coefficient (in %) as a function of d, for $\epsilon_r = 2.1$.

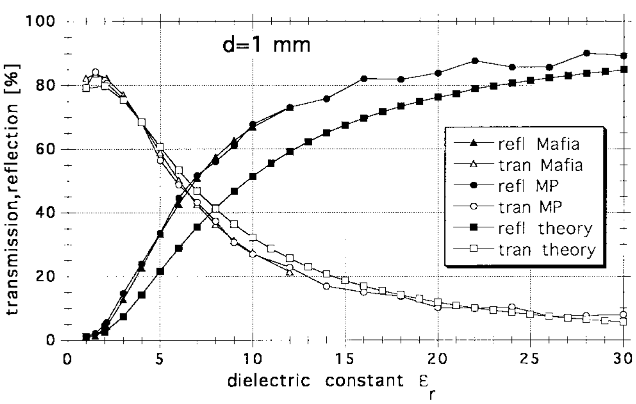

Fig. 5. Comparison of transmitted and reflected power for a normal gap. ($d = 1$ mm).

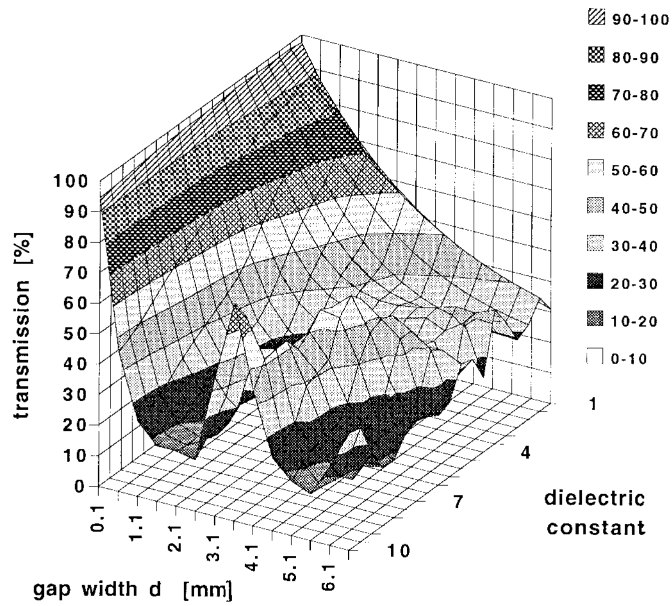

Fig. 6. The transmission as computed by a numerical code. Note that the greater the gap length or the dielectric constant, the less wave is transmitted.

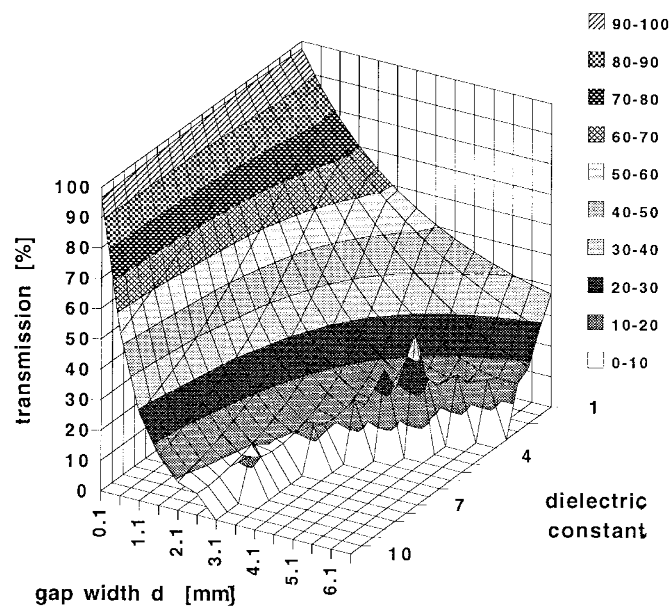

Fig. 7. The transmission as computed by analytical theory. The region where theory is no longer defined (because k_1 becomes imaginary) was filled with zeros (flat plateau in the front).

Concerning the sum of reflection and transmission, we note that it is still physically consistent, that is, it does not exceeds one even for large value of ϵ_r.

In Fig. 6 we plot a 2-D histogram of transmission as computed the MP code. Note that the greater the gap width or the dielectric constant, the less wave is transmitted, until some undulation (shown in front view) appears between 20–50%. In Fig. 7 the 2-D histogram for analytically computed transmission is shown for comparison. The flat zero plateau in the front is where theory is no longer defined (because k_1 become imaginary). The region of criterion (41) correspond roughly the first six bands of histogram (corresponding to transmission greater than 40%). In this region, agreement between theory and results is fairly good.

Having obtained an analytical solution from first principles of a 2-D dc break, discrepancies with numerical results may come only from approximations used; and the only approximation used here is neglecting all poles $\ell \geq 2$ on the ground that they contribute less than k_1 and k' poles because they are far away from real axis. It should be noted that the inclusion of $\ell = 2, 3$ poles in X function computation will be extremely laborious, albeit possible. On the other side $l = 2$ pole can be easily included in Z, but it proved to be practically irrelevant.

We also note that in the limit $d \to 0$ the agreement between theory and codes becomes very good. This can be expected, since the poles $k_y = ik_\ell$ move toward infinity, therefore making the $\ell = 1$ truncation more plausible.

ACKNOWLEDGMENT

The authors wish to thank Dr. G. Mourier of Thomson Tubes Electroniques for many valuable discussions. The kind support of Dr. A. Wien and Prof. Dr. M. Thumm of the University of Karlsruhe in providing MAFIA simulations is greatly appreciated.

REFERENCES

[1] R. Geller, "Electron heating in ECRIS," in *Proc. 11th Int. Workshop Electron Cyclotron Resonance Ion Sources (ECRIS 11)*, Univ. of Gröningen, The Netherlands, May 6–7, 1993, pp. 1–17.

[2] V. Bechtold, H. Dohrmann, and S. A. Sheikh, "A highly efficient ECR ion source for radioactive beams," in *Contributed Papers of the 7th Workshop Electron Cyclotron Resonance Ion Sources,* Kernforscunganlage Jülich, Germany, May 22–23, 1986, p. 248–257.

[3] B. Jacqout, P. Briand, F. Bourg, and R. Geller, "Source d'ions lourds Caprice 10 GHz $2\omega_{\rm ce,}$" *Nuc. Instrum. Methods*, vol. A 269, p. 1–6, 1988.

[4] M. Mongiardo and T. Rozzi, "Singular integral equation analysis of flange-mounted rectangular waveguide radiators," *IEEE Trans. Antennas Propagat.*, vol. 41, pp. 556–565, 1993.

[5] T. Weiland, "Numerical solution of Maxwell's equations for static, resonant and transient problems," *U.R.S.I. Int. Symp. on Electromagnetic Theory*, Budapest, Hungary, Proc. Part B, pp. 537–542, 1986.

[6] M. Koshiba, M. Sato, and M. Suzuki, "Application of finite-element method to H-plane waveguide discontinuities," *Electron. Letts.*, vol. 18, pp. 364–365, 1982.

[7] J. P. Webb, G. L. Maile, and R. L. Ferrari, "Finite-element solution of three-dimensional electromagnetic problems," *Proc. Inst. Elect. Eng.*, vol. 130, pt. H, pp. 153–159, 1983.

[8] S. Kagami and I. Fukai, "Application of boundary-element method to electromagnetic field problems," *IEEE Trans. Microwave Theory Tech.*, vol. 32, pp. 455–461, 1984.

[9] M. Koshiba and M. Suzuki, "Application of the boundary-element method to waveguide discontinuities," *IEEE Trans. Microwave Theory Tech.*, vol. 34, pp. 301–307, 1986.

[10] E. Kühn, "A mode matching method for solving field problems in waveguide and resonant circuits," *Arch. Elek. Übertragung*, vol. 27, pp. 511–518, 1973.

[11] L. Lewin, *Theory of Waveguides.* London, UK: Newnes-Butterwoths, 1976.

[12] F. Arndt, I. Ahrens, U. Papziner, U. Wiechmann, and R. Wilkeit, "Optimized E-plane T-junction series power divider," *IEEE Trans. Microwave Theory Tech.*, vol. 35, pp. 1052–1059, 1987.

[13] L. Lewin, "On the inadequacy of discrete mode-matching techniques in some waveguide discontinuity problems," *IEEE Trans. Microwave Theory Tech.*, vol. 18, pp. 364–372, 1970.

[14] K. H. Park and H. J. Eom, "An analytic series solution for H-plane wave-guide T-junction," *IEEE Microwave Guided Wave Lett.*, vol. 3, pp. 104–106, 1993.

[15] L. S. Sheingold and J. E. Storer, "Circumferential gap in a circular wave guide excited by a dominant circular-electric wave," *J. Appl. Phys.*, vol. 25, pp. 545–552, 1954.

[16] N. Morita and Y. Nakanishi, "Circumferential gap in a $\rm TE_{01}$ mode transmitting multimode circular waveguide," *IEEE Trans. Microwave Theory Tech.*, vol. 16, pp. 183–189, 1968.

[17] R. E. Collin, *Field Theory of Guided Waves.* New York: McGraw-Hill, 1960.

Christos T. Iatrou was born in Elefsina, Greece, on April 19, 1962. He received the Dipl. Eng. degree from the Department of Electrical Engineering, University of Patras, Greece, in 1986 and the Ph.D. degree from the Department of Electrical Engineering, National Technical University of Athens, Greece, in 1990.

From 1990 to 1992 he held a Post-Doctoral appointment at Thomson Tubes Electroniques, Velizy, France, where he worked on the theory of gyroklystron amplifiers and the development of quasi-optical mode converters for gyrotrons. From 1993 to 1993 he was Research Fellow at the National Institute of Nuclear Physics (INFN), Legnaro, Italy, where he worked on the development of an electron cyclotron resonance ion source. Since October 1993 he has been with the Research Center (Forschungszentrum) Karlsruhe, Germany, working on the development of high power gyrotron oscillators. His research interests are focused on the physics of electron beam devices, such as gyrotrons, gyroklystrons, harmonic gyrotrons, and slow-wave electron cyclotron masers.

Marco Cavenago was born in Vimercate, Italy, on April 24, 1961. He earned the Laurea degree in physics from Pisa University in 1984 and received the Ph.D. degree in physics from Scuola Normale Superiore in 1987, discussing new techniques in particle acceleration and instabilities in betatrons. He worked on the same subjects at University of California, Irvine, in 1985–1986.

Since 1988, he has worked with the Laboratori Nazionali of Legnaro, Italy, a branch of Istituto Nazionale di Fisica Nucleare, where he built an Electron Cyclotron Resonance ion source and is completing a high voltage platform. His researches interests are focused on mathematical physics of particle acceleration, plasma physics, and accurate design of electromagnetic devices of ion sources: magnets, einzel lenses, and microwave components.